A framework for behaviour quantification vis-a-vis adoption of public policy measures - lessons from nonpharmaceutical measures during COVID-19

Sarah Smook[a], Lia Humphrey[a], David Lyver[a], Zahra Mohammadi[a], Rhiannon Loster[a], Ed Thommes[a,1], Monica Cojocaru[a]

[a]*Department of Mathematics & Statistics, University of Guelph, Guelph, ON, Canada*
[b]*Sanofi Pasteur...*

Abstract

In this work, we provide estimates of non-pharmaceutical interventions (NPIs) adoption and its effects on the COVID-19 disease transmission across the province of Ontario, Canada in 2020, used as a case study. Using a multilinear regression process, we estimate a perceived risk of infection and a personal discomfort of complying with NPIs for Ontarians across 34 public health units. With the use of game theory, we model a time series of decision making processes by which we estimate how average individuals in each public health region decide to adopt NPIs. This model gives an expected NPI adoption level across Ontario from March to December 2020. Using an SEIRL compartmental model for ON, we are able to estimate a province-wide effectiveness level of NPIs. Last but not least, we show the model's versatility by: a) applying it to other parts of the world; b) using it in counterfactual scenarios in case of future emerging infections.

Keywords: COVID-19; non-pharmaceutical interventions; game theory and decision making models; Nash equilibrium; behavioural epidemiology; infectious disease.

1. Introduction

Rapid worldwide spread of the novel coronavirus SARS-CoV-2 and its related disease COVID-19 quickly shifted the priorities of public health experts and policymakers in early 2020. Despite strict initial protective measures applied in Canada, such as the closure of borders and non-essential

services [1], new cases continued to sweep across provinces. For a novel pathogen with unidentified transmission dynamics, a population's behaviour is a significant factor in predicting the spread of infection, which can inform health policies such as resource allocation or regional guidelines. However, many existing mathematical models do not adequately represent the relation between individual decision-making and disease prevalence that occurs in a rapidly evolving public health crisis like a pandemic [9]. Personal values and perceived transmission risk to individuals played a large role in the evolution of the COVID-19 pandemic in Canada, a better understanding of which could help decision makers to model improved disease mitigation strategies in the future. In this paper, we investigate non-pharmaceutical control measures adoption in the province of Ontario (and in the US states of Georgia and Pennsylvania), and use a game theoretic framework to infer how NPIs adoption influenced the outcomes across the regions, and at what levels of efficacy.

2. Background

On January 25^{th}, 2020, the first positive case of COVID-19 in Canada was reported in Toronto, Ontario [5]. In absence of pharmaceutical prophylactic options, the national number of reported cases rose to nearly 10,000 by the end of March [30], at which point the Public Health Agency of Canada began recommending and later mandating the implementation of non-pharmaceutical interventions (NPIs) to reduce and delay further contact transmission events, including social/physical distancing, shelter-in-place or "lockdown" periods, service closures, intensified sanitation procedures, and face masks [43, 1]. However, even recent Canadian pandemic planning guidance notes that the impact and limitations of such NPIs in an outbreak situation were still not well studied leading up to 2020 [12]. While the success of a public health intervention is known by epidemiologists to depend upon adherence by the target population, the COVID-19 response presents an opportunity to further investigate the spatiotemporal factors affecting individuals' behaviour and decisionmaking regarding NPIs during a pandemic.

Mathematical modeling has come a long way in terms of utility for public health planning and policy, thanks in part to the extension and refinement of seminal works like the Kermack-McKendrick Susceptible-Infected-Recovered (SIR) compartmental model as well as the sophistication of modern data and computing abilities. For example, in [22], the authors implemented addi-

tional quarantine and isolation compartments and highly detailed population contact rates (developed by [40]) to simulate early COVID-19 transmission in Ontario. However, even the most detailed of contact patterns represent population averages that occur under "normal" conditions and cannot be assumed static in the context of epidemic modelling [19]. Moreover, deviations from behavioural norms are rarely uniform across entire populations in extreme circumstances [50]. Growing evidence from recent public health crises (e.g. 1980s HIV/AIDS, 2003 SARS, 2009 H1N1) demonstrates that people's behaviour evolves with the epidemic progression as they respond to new information and form perceptions of risk (see for example: [29, 28, 42, 20, 35, 46]). The sum of these factors may result in underestimated pandemic effects and motivates further refinement of human behaviour modelling in epidemic simulation models.

Earlier works approached behaviour and transmission as having a cause and effect relationship, whereby one is modelled operationally and the other as a basis to interpret the results [9]. For example, [13] was the first to vary the contact rate β over time according to disease prevalence, so that a rise in infection risk would result in a decrease in population mobility. These ideas lead to "behavior-incidence" models that incorporated both behaviour and transmission submodels as complementary inputs to better reflect real-world dynamics [9, 47]. Dynamic adjustments to contact rates remain a common technique for modelling NPI-related behavioural changes across many infectious diseases, though there are differences involving the degree of heterogeneity in population characteristics and the number of strategies considered; the COVID-19 modelling challenge was no exception. One 2020 study used an economic-based optimization approach coupled with a compartmental model where the proportion of individuals voluntarily adopting NPIs changed depending upon their age-based risk of mortality and the time-varying disease prevalence [44]. Another considered differences in NPI compliance simultaneously by allowing for interaction of individuals with behaviour-varying likelihoods of infectiousness [8].

Game theoretic models [48] have become an attractive behavioural pairing to disease transmission models, providing a framework to view a population as being made of a group of individuals ("players") who make strategic decisions to try and maximize their own health benefits during a public health threat, while also being influenced by the decisions of others. The point where no player can further improve their outcome by choosing a different strategy is called a Nash equilibrium, and is the most common way to define

the solution to a non-cooperative game involving two or more players [38]. Game theory has seen prominent application in voluntary vaccine uptake models [11, 10, 16, 18, 27], and to a lesser extent NPIs [46].

3. Materials and methods

In this work, we design a population game to serve as a behavioural model which is paired with a previous compartmental transmission model for COVID-19 used in ([26, 22, 33]). The game model helps to investigate spatio-temporal population adherence to NPI mitigation measures across the province of Ontario, Canada in 2020 (where Ontario is used as our case study), whereas teh pairing between teh game and the transmission model is used to infer efficacy of NPIs over time in Ontario. It is important to differentiate here a game model from traditional decision models where individuals simply optimize their well-being, or minimize their cost, without allowing for influence from the decisions of others.

COVID-19 data were coordinated across Ontario's 34 public health units (PHUs), which are responsible for the delivery of local health services and whose jurisdictions are generally partitioned according to census municipalities [31]. At this level of data stratification, we seek the monthly Nash equilibrium across each PHU from March 1^{st} to December 31^{st} 2020, representing an Ontarian's monthly likelihood of adopting NPI measures in a given PHU while subject to local and provincial influence and information. WE also deduce biweekly levels of efficacy of NPIs over time.

3.1. Transmission model

Following [33], COVID-19 transmission in Ontario is simulated via an SEIRL (Susceptible, Exposed, Infectious, Recovered and isoLated) model with daily incidence data across Ontario and at the PHU level. This model assumes that the population is homogeneous and well-mixed, that infected individuals are either symptomatic or asymptomatic, and that most individuals who are aware of their infection isolate for a fixed period of time. The system is described with the following ordinary differential equations:

$$
\begin{cases}
\dfrac{dS}{dt} = -\beta S(t)\dfrac{I(t)}{N_{total}}, \\
\dfrac{dE}{dt} = \beta S(t)\dfrac{I(t)}{N_{total}} - \sigma E(t), \\
\dfrac{dI}{dt} = \sigma E(t) - \gamma I(t) + \epsilon(\gamma - \kappa)(1-a)I(t) \\
\dfrac{dL}{dt} = \epsilon\kappa(1-a)I(t) - \gamma L(t). \\
\dfrac{dR}{dt} = \gamma(1-\epsilon(1-a))I(t) + \gamma L(t).
\end{cases} \tag{1}
$$

Our model parameters (Table 1) have been taken from literature, with the exception of the proportion of infected who isolate, ϵ, which we assume to be equal to 95%, and the isolation rate κ.

Symbol	Definition	Initial Value	Reference
N_{total}	Population size	Table 4	
σ	Rate at which exposed become infectious (days^{-1})	1/2.5	[45]
a	Proportion of permanently asymptomatic cases	0.5	[32],[25],[36]
ϵ	Proportion of compliance with isolation	0.78	[17]
κ	Isolation rate	1	assumed
γ	Recovery/removal rate	1/7	[49]

Table 1: Parameter values for our model 1.

3.2. Behavioural model - regional perceived personal NPIs discomfort and perceived personal risk of infection

In this section we construct parameter inputs we need to formulate the NPIs adoption game. In what follows, we define Ontario's Public Health (PH) regions as a group of players competing to minimize personal risks of getting infected with Covid-19 as well to minimize personal discomfort with adoption of NPIs. Each PH region is thought of a set of identical players, where players' decisions at any given time are interdependent. The choice of one player to adopt NPIs provides a net positive health payoff for others by reducing COVID-19 transmission risk, but in turn it may incentivize another player not to use NPIs and still benefit from the conferred protection. Since both options are available at each time step across the population, players face uncertainty and make use of available information to assess their personal risk. The concepts of free ridership and information signaling are well studied in vaccine game literature [**?**]

We assume that time-varying individual decisions regarding NPIs are affected by both personal discomfort incurred from NPIs adoption (denoted by

$\tilde{r}$) and by the personal perceived risk of getting infected when not adopting NPIs (denoted by $\bar{r}$). Let us define and discuss these two parameters more in depth.

To quantify $\bar{r}$ and $\tilde{r}$, we set up two multivariable linear regressions (MLR) per PHU per month to express each in terms of relevant empirical data. First, we collected daily reported counts of COVID-19 incidence and deaths by PHU. Such information was broadcast daily by major provincial news bodies and their regional affiliates (e.g., CBC, CTV News, Ontario Newsroom) via television and the internet to provide ongoing coverage of the pandemic and related developments. Similarly, we collected daily COVID-19-related hospitalizations, but at the province level instead of by PHU. The decision was based partly on reporting trends by news agencies, but also Ontario's disproportionate population density and concentration of hospital facilities. For example, the Northern health region, encompassing 7 of 34 PHUs and 88% of Ontario's landmass, serves just 6% of the province's population and hosts 47 of 141 hospital sites [4, 7, 37]. Additionally, overwhelmed hospitals coordinated patient transfers to accommodate for the sheer volume of severe COVID-19 cases [39], making it difficult to track cases by PHU of origin. We assume that the overall daily number of hospitalizations in Ontario better reflects the severity of the COVID-19 situation that would factor in to an individual's personal risk perception than their local hospital numbers.

Based on the wide availability of the above information in easy access formats, we assume that these figures define an average Ontarian's understanding of the severity of their local and provincial pandemic situations at given time points. By including these data, we can achieve an effect similar to evolutionary vaccination games [], whereby individuals continually assess their approach to NPIs by considering past and current COVID-19 information.

Second, we examined daily population mobility changes across all PHUs as a proxy for community contact reduction reflecting voluntary and government-mandated risk avoidance measures before and after the onset of COVID-19. We utilize the *COVID-19 Community Mobility Reports* made available by Google [3] that tracked and partitioned cellphone mobility data according to the following five indicators: Grocery and pharmacy stores, parks, transit stations, retail and recreation and workplaces. Each indicator is calculated as frequency of visits relative to activity during the baseline time period, defined as the median of the corresponding day of the week between January 3 to February 6, 2020. More information regarding the Google mobility

data and how it was partitioned according to the PHUs can be found in the Appendix **??**.

Third, to examine the individual effects of government-mandated health policies, we used the Oxford COVID-19 Government Response Tracker (Ox-CGRT) which was created to collect and standardize information on COVID-19 government policy measures in over 180 countries and provide tools to compare and measure their impacts [24]. We focus specifically on the Ox-CGRT Stringency Index, which measures the strictness of "lockdown" policies that primarily restrict regular activities and mobility. This data was available at the provincial level. +++

Estimation of perceived risks of infection, as well as personal discomfort with mask use, are in general a difficult problem which necessitates further assumptions alongside available data. In our case here, we will use a combination of regional ($_R$) and province-wide ($_P$) freely available data on incidence, hospitalizations, Oxford index, Google mobility index and observed mask use. Further, we will assume that the observed level of mask use in a regional population is proportional with personal discomfort, while the remaining (Google) work mobility in a region is proportional with the personal perceived risk of infection for an average individual in a PH. Last but not least, we will assume a linear relationship between observed mask use (as dependent variable), cases and Oxford index on one hand (as independent variables), and another linear relation between the reduced work mobility (as dependent) and cases and hospitalizations (as dependent variables). In other words, we assume to have:

$$G_{work-mobil}(t) = v_1(cases(t)) + v_2(hospitalizations(t)) + \bar{r_i}(t), \qquad (2)$$

where $\bar{r_i}$ is the value of the work-related mobility in the absence of new COVID-19 cases and hospitalizations. We then assume that the personal perceived risk of infection is proportional to the this value: this means that when work-related mobility decreases, the perceived risk should decrease, and vice-versa.

Similarly, we assume that

$$M_{observed}(t) = w_1(cases(t)) + w_2(OxCGRT(t)) + \tilde{r_i}(t) \qquad (3)$$

where $\tilde{r_i}$ is the value of the observed mask use in the absence of cases and

absence of economic measures. We then assume that the personal discomfort with wearing a mask is proportional to the this value: when mask wearing levels are observed to increase, the discomfort should increase, and vice-versa.

Both computations for $\bar{r_i}$ and $\tilde{r_i}$ capture very broad cases which are sufficient for our research, however possibilities for further refinement are discussed in our Discussions section 6. Regression analysis was computed using the statistical software R's *lm* function which is used for fitting linear models. We repeat for each PHU, collecting the perceived risk of infection and personal discomfort terms into the $\bar{r_i}$ matrix and $\tilde{r_i}$ matrix respectively. where $\bar{r_i}(t)$ for $i \in \{1, 2, \ldots, 34\}$ represents the corresponding PHU via column, and $t \in \{1, 2, \ldots, 10\}$ is the monthly time step starting from March to December of 2020.

There are some interesting insights that we could highlight in the evolution of perceptions over time. For instance, in Figure 1 we depict the evolution of the risk of infection in the PH regions of Algoma, North Bay Parry Sound, Northwestern, Sudbury, Renfrew, Thunder Bay, and Timiskaming, which are some of the lowest density populated regions of ON (upper panel, versus the regions of Durham, Halton, City of Hamilton, Niagara, Ottawa, Peel, Waterloo, York, Toronto, which are some of the highest populated (lower panel). We see that there are differences in this evolution ....

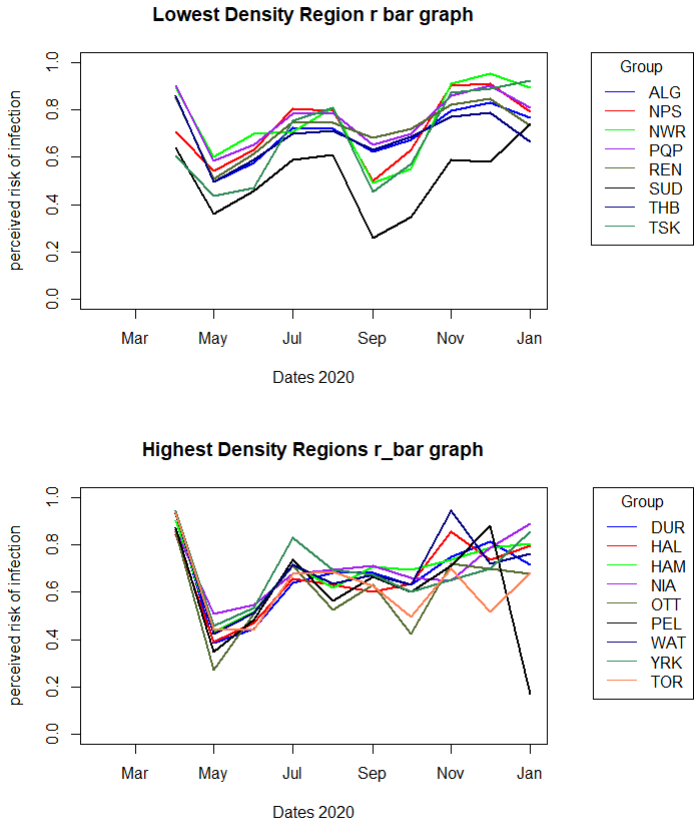

Figure 1: Caption

A similar plot is presented in Figure 2, where we see the perceived discomfort with mask wearing among the two subpopulations. Interestingly....

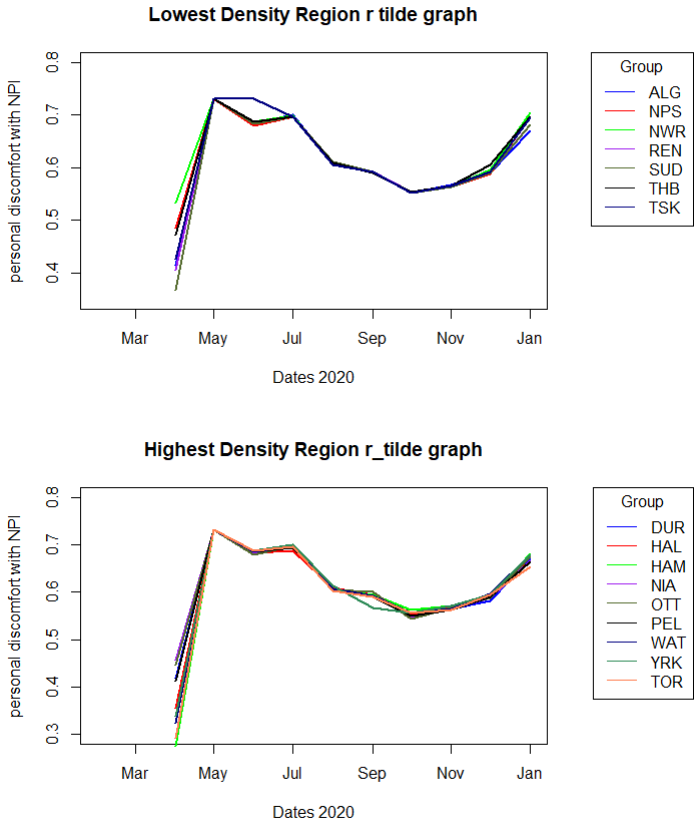

Figure 2: Caption

Last but not least, we looked at some socio-economic and demographic factors and their possible relation to how the population perceived the NPI's. We found that there are some correlations here, probably due to mobility and incidence, ...(see Figure 3)

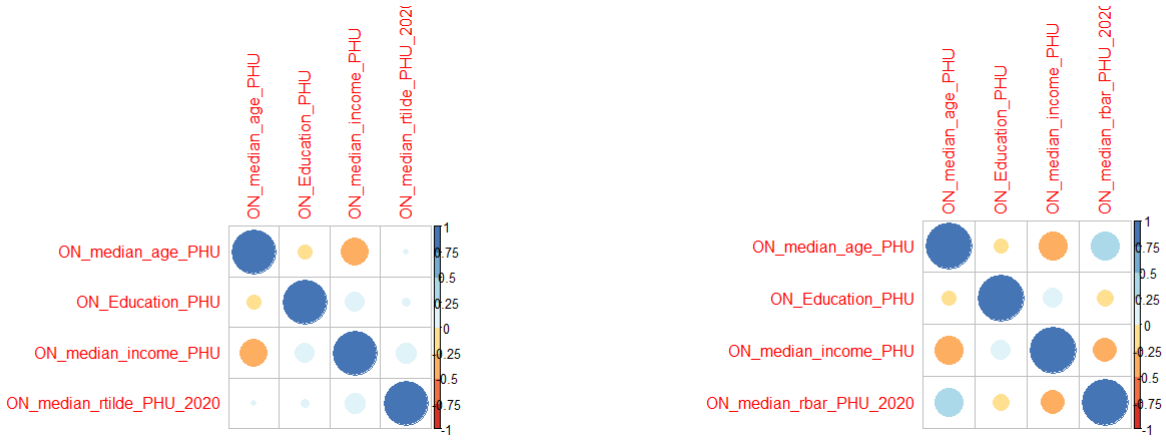

Figure 3: There is somewhat of a positive correlation between median age and the perceived risk of infection, and a somwhat negative correlation between median income and the perceived risk of infection (right panel). There are no correlations of these factors with the personal discomfort (left panel).

4. The NPI adoption game

Our model has 34 interacting groups whose decisions affect each other's perceived relative risk of infection. That is to say we have a game taking place between population groups. For ease of reading, An n-person game is one in which each player has a finite set of pure strategies and a definite set of payments to the n players which correspond to each n-tuple of pure strategies, one strategy being taken for each player [34]. Mixed strategies are probability distributions over the pure strategies with payoff functions as the expectations of the players. Hence mixed strategies take polylinear forms in the probabilities with which the various players play their pure strategies [34]. A Nash equilibrium is an outcome from a game in which once achieved, no player can increase their payoff by switching strategies [34]. If most of the population adopts strategy P and individuals who adopt another strategy Q always obtain a lower payoff than those adopting P, then P is said to be a Nash equilibrium. If most individuals adopt strategy Q however, individuals adopting a strategy that is closer than Q to P obtain a higher payoff for any $Q \neq P$, then P is said to be convergently stable. If P is a Nash equilibrium and all payers are currently playing P, then no one should change strategy. If P is convergently stable, then regardless of what strategy is most common in the population, individuals should start to play strategies closer to P and

ultimately adopt P. It is generally expected that a strategy observed in a real population must be a convergently stable Nash equilibrium.

A multiplayer Nash game consists of a finite number of players denoted by $N > 0$. A generic player $i \in \{1, \ldots, N\}$ has a strategy vector x_i selected from a closed convex set $S_i \subset \mathbb{R}^{n_i}$ so that $n_1 + \cdots + n_N = n$. A player has a payoff function $u_i : K \longrightarrow \mathbb{R}$, where $K \coloneqq S_1 \times \cdots \times S_N$ or the cross product of the strategy sets of all players; evidently: $K \subset \mathbb{R}^{n_1 + \ldots + n_N = n}$. In general we strive to find a Nash equilibrium strategy vector $\underline{x^*} \coloneqq (x_1^*, x_2^*, \ldots, x_N^*)$, such that when player $i \in \{1, \ldots, N\}$ plays x_i^*, there is no reason to switch strategies and as such, these strategies should be stable equilibrium solutions of our game. Mathematically, we define a Nash vector of strategies as follows:

Definition 1. *Assuming each player is rational and wants to minimize their payoff function $u_i : K \longrightarrow \mathbb{R}$. Then a* ***Nash equilibrium*** *is a vector $x^* \in K$ which satisfies the inequalities:*

$$u_i(x_i^*, \hat{x}_i^*) \leq u_i(x_i, \hat{x}_i^*), \ \forall i \in \{1, \ldots, N\}, \ \forall x_i \in S_i, \ \textit{where}$$

$$\hat{x}_i^* \coloneqq (x_1^*, \ldots, x_{i-1}^*, x_{i+1}^*, \ldots, x_N^*)$$

First, let $\bar{r}$ be the perceived personal risk of COVID-19 infection to an individual, which may be affected by a mixture of personal beliefs, the choices of others, and empirical prevalence data. Second, let $\tilde{r}$ be the personal discomfort to an individual when complying with mandated NPIs, which reflects factors such as convenience and precaution fatigue. We then denote by $r_i(t)$ the relative perceived risk estimate of an individual residing in one of the 34 PHUs, defined as the ratio of these two factors:

$$r_i(t) = \frac{\tilde{r_i}(t)}{\bar{r_i}(t)}, \quad \forall i \in (1, 2, \ldots, 34), \quad t > 0. \tag{4}$$

That is to say, whenever the relative risk exceeds 1, the personal discomfort with measures is higher that the perceived risk of infection, and vice versa.

For simplicity, we assume that all residents in a given PHU are provided with the same information and use this information to asses their risks and discomforts. We let $N = 34$ and $i \in \{1, \ldots, 34\}$, representing an average player (resident) in each of the 34 PHUs in Ontario. The population of each PHU represents a fixed proportion of the total Ontario population ϵ_i,

where $\epsilon_i \in (0,1)$ and $\sum_{i=1}^{34} \epsilon_i = 1$. Players of different PHUs will have different perceived risks of infection ($\bar{r_i}$) and personal discomfort with NPIs ($\tilde{r_i}$). Recall that $r_i \coloneqq \frac{\tilde{r_i}}{\bar{r_i}}$ is the relative perceived risk of adopting NPIs. The strategy of any player $i \in \{1, \cdots, 34\}$ is the probability that they will adopt NPIs, denoted by $x_i \in [0,1]$, hence the strategy set for our game will be $K \coloneqq [0,1] \times \cdots \times [0,1]$.

To define payoffs to each player, we adapt a utility function that was previously used to determine Nash equilibrium solutions for well-studied vaccine-preventable childhood diseases from [11, 16]:

$$U_i(t) = r_i x_i(t) + \Big(1 - \delta_i(t) \cdot \sum_{i=1}^{34} \epsilon_i x_i(t)\Big)\Big(1 - x_i(t)\Big),\ \forall t \in \{1, \cdots, 10\} \quad (5)$$

In this setting, U_i represents the agent's disutility (or cost) of disease prevalence as a function of total population NPI compliance (given by $\sum_i \epsilon_i x_i$), as well as the efficacy of the enforced NPI's. A greater perceived coverage in the population means a reduced perceived infection risk for susceptible individuals. In general, $\delta_i(t)$ signifies the perception of player i on the overall adoption of NPI measures in the province, and it is not something we can estimate from the decision model, rather we rely on it to solve the game. Since it is a quantity very difficult to measure, we will solve our decision model using a statistically uniform spread of values of $\delta_i(t)$, for each i and t, thus generating an envelope of NPI adoption curves for each region and for ON.

To reflect the expected contribution of the NPI measures we consider here on the reduction of transmission of COVID-19, we further use the epidemiological model for ON (Section 5 below).

Therefore we first solve the game:

$$\min_{x_i} U_i(x) = r_i x_i(t) + \Big(1 - \delta_i(t) \sum_{i=1}^{34} \epsilon_i x_i(t)\Big)\Big(1 - x_i(t)\Big)$$

$$\text{s. t. } 0 \leq x_i(t) \leq 1$$
$$\delta_i(t) \in [0,1] \text{ for each } i \in \{1, 2, \ldots, 34\} \text{ and for each fixed } t \in \{1, \cdots, 10\} \quad (6)$$

for the mixed Nash equilibria x_i^* for each PHU in Ontario. Each x_i^* represents

a given player in region i's probability of respecting NPIs. We use a projected dynamical systems (PDS) approach to gain greater analytic capabilities, including the ability to visualise the structure of the dynamic game through theoretical analysis, as well as compute the optimal strategy and respective equilibrium NPI compliance likelihoods [16]. Using MATLAB we solve: With these regional probabilities, we are able to determine the *expected NPI-adoption level for Ontario*, namely: $eNPI_{adopt} := eff_{NPI} \sum_{i=1}^{34} \left(\epsilon_i x_i^*(t)\right)$. We present the determined $eNPI_{adopt}$ for ON in Figure 4:

Figure 4: Weekly expected NPI adoption across Ontario from March to December 2020; note that for the first 2 weeks of March 2020, the adoption levels are 0.

5. Efficacy of adopted measures as a fraction of transmission reduction in ON

In this section we investigate the use of non-pharmaceutical interventions on disease transmission. Since our estimated $eNPI_{adopt}(t)$ should be meaningful vis-a-vis the evolution of the transmission, we modify the SEIRL model of Section 3.1 to incorporate a time dependent transmission rate

$$\beta(t) = \beta_0(1 - eNPI_{adopt}(t)), \tag{7}$$

as in [33], where β_0 is the value of the transmission in March 2020 (near disease-free equilibrium). We express the time changing β as a function of the exponential growth of the SEIRL model above as:

$$\beta(\rho) = \frac{\epsilon\gamma a\rho + \epsilon\gamma a\sigma - \epsilon\kappa a\rho - \epsilon\kappa a\sigma - \epsilon\gamma\rho - \epsilon\gamma\sigma + \epsilon\kappa\rho + \epsilon\kappa\sigma + \gamma\rho + \gamma\sigma + \rho^2 + \rho\sigma}{\sigma} \tag{8}$$

To estimate the exponential growth factor for ON as a time series, we rely on weekly case incidence data (which we denote by $inc(t)$) for each region. We assume that $inc(t)$ is given by an exponential curve of the type (see [33, 26]):

$$inc(t) = inc(0)e^{\rho t}.$$

In this case, we can compute a time-series of the exponential growth factor:

$$\rho(t) = \ln \frac{inc(t+1)}{inc(t)}, \text{ with } inc(t) \neq 0.$$

We have the following weekly picture for ON:

Figure 5: $\beta(t)$ across Ontario from March to December 2020

By comparing the two times series realizations for the transmission rate β, given by (7) and (8), we can analyze the difference:

$$\xi(t) := \|\beta(\rho) - \beta_0(1 - eNPI_{adopt}(t))\|,$$

with $\beta(\rho)$ given by (8), and where $\xi(t)$ is a quantity representing the overestimation or underestimation of transmission dynamics offered by the behavioural decision model in ON.

Figure 6: Weekly transmission reduction in ON due to individual decisions versus transmission reduction estimated from data across Ontario from March to December 2020

5.1. MODEL APPLICATION - other regions

To demonstrate the versatility of our mathematical framework (game + epidemiological model), we demonstrate below how we applied it to two other similar regions, this time in the United States: Pennsylvania and Georgia. Table **??** below includes the characteristics of these two states, and their distinctions from the Ontario case.

	Population	Health Regions
ON	14 mil.	34
PA	12 mil.	6
GA	10.6 mil.	18

Table 2

In a similar manner, we estimate the expected adoption levels of NPI in PA and GA, from March 2020 to December 2020, and we plot them in Figure 7 below. Note that ....

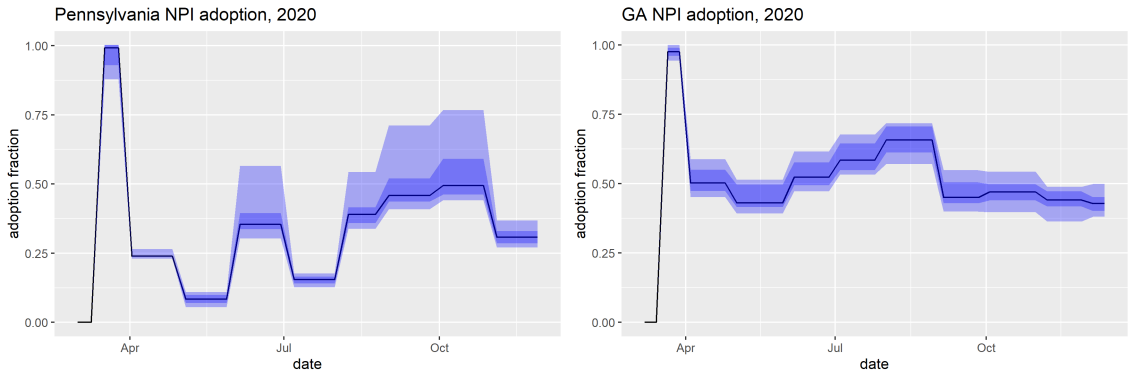

Figure 7: Weekly expected NPI adoption across PA (left) and GA (right) from March to December 2020; note that for the first 2 weeks of March 2020, the adoption levels are 0.

Following from here, we estimate the decision model transmission rates versus the observed transmission rates for each state:

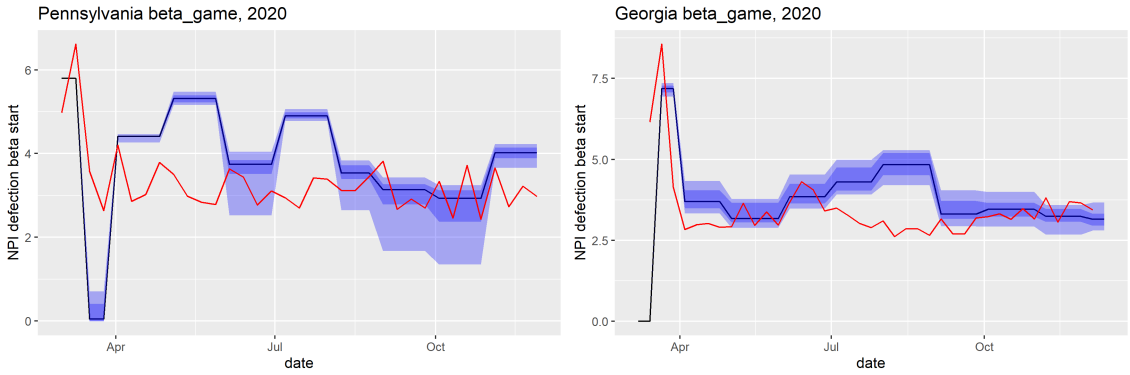

Figure 8: PA and GA transmission rates estimates from decision model and incidence

5.2. MODEL APPLICATION (Countries)

This model can be applied to a variety of different regions around the world in which the necessary data is made available. To apply this model, Google mobility reports and the Oxford Index would have to be available by province or state within the country, as well as the COVID-19 case numbers would have to be available by regions within the provinces or states, similarly to Ontario's public health units. This would be useful in comparing how differences in public health policies affected risk perception in within these countries. Some examples that could be explored include Australia, Brazil, India, and the United Kingdom.

Unlike Ontario, Australia closed both its internal and external borders, as well as mandated, rather than advised, self-isolation for 14 days for travellers. [41] The Australian government was also much faster than Ontario at locking down long-term care homes from outside visitors.[41] With available COVID-19 case data available from the Australian Government Department of Health, Google Mobility reports by regions, and the Oxford Stringency Index also available by region, this model can be applied to any number of regions within Australia.

The Brazilian Government public health policies differed greatly compared to Ontario's throughout 2020. [21] The President of Brazil did not acknowledge the seriousness of COVID-19 and even tried to undermine local municipal authorities that tried to implement policies to help reduce the spread of the disease. [21] This led to much worse epidemiological curves and higher mortality rates within the country. Brazil also has available case data from the Brazilian Ministry of Health, regional Google Mobility reports, and the Oxford Stringency Index by region.

India had one of the strictest lockdowns in the world starting at the end of March 2020, which is much more strict compared to Ontario's voluntary lockdown, however, India still suffered high mortality rates in both the first and second wave of the pandemic. [23] Using available case data from the Government of India, regional Google Mobility reports, and the Oxford Stringency Index by region, to apply this model to regions within India, could give some understanding as to the high case numbers despite the strict policies implemented in the country.

Lastly, the United Kingdom has many similarities to Canada and faced many common challenges like acquiring PPE and struggling to increase available testing. [2] The United Kingdom also implemented policies differently in reaction to the pandemic, one of which was a national mandate for lockdown, rather than the voluntary lockdown in Ontario. [2] The data needed to apply this model for regions within this country is also available, including COVID-19 case data from both the Government of the United Kingdom and the Scottish Government, as well as regional Google Mobility reports, and the Oxford Stringency Index by region.

6. Discussion

Need to add.

- incidence/deaths/hospitalizations were based on daily reported cases as that was the information made available to the public daily; the real adjusted and unreported numbers could have been higher : verify

- the underlying SEILR transmission model assumes 95% isolation compliance (ϵ) and 1-day isolation rate, which are not necessarily realistic (Add here the citation from Zhara for ON = 78%; I ran PA and GA with 70% isolation rates in the beta plots above)

7. Conclusion

Need to add. Mention plan to incorporate vaccination in next manuscript.

References

[1] Canadian covid-19 intervention timeline.

[2] A comparison of 2020 health policy responses to the covid-19 pandemic in canada, ireland, the united kingdom and the united states of america.

[3] Google COVID-19 Community Mobility Reports.

[4] 2016 Census Profile.

[5] COVID-19 cases, hospitalizations and deaths in Ontario — CTV News, March 2020.

[6] Table 22-10-0143-01 Smartphone personal use and selected smartphone habits by gender and age group, June 2021.

[7] 2021 Census of Population. Statistics Canada Catalogue no. 98-316-X2021001.

[8] Barbarossa, M. V., and Fuhrmann, J. Compliance with npis and possible deleterious effects on mitigation of an epidemic outbreak. *Infectious Disease Modelling 6* (2021), 859–874.

[9] Bauch, C., d'Onofrio, A., and Manfredi, P. Behavioral epidemiology of infectious diseases: an overview. *Modeling the interplay between human behavior and the spread of infectious diseases* (2013), 1–19.

[10] Bauch, C. T. Imitation dynamics predict vaccinating behaviour. *Proceedings of the Royal Society B: Biological Sciences 272*, 1573 (2005), 1669–1675.

[11] Bauch, C. T., and Earn, D. J. Vaccination and the theory of games. *Proceedings of the National Academy of Sciences 101*, 36 (2004), 13391–13394.

[12] Canada, H., 2019.

[13] Capasso, V., and Serio, G. A generalization of the kermack-mckendrick deterministic epidemic model. *Mathematical biosciences 42*, 1-2 (1978), 43–61.

[14] Ceci, L. Top U.S. mapping apps by downloads 2021, February 2022.

[15] Cheung, C., Lyons, J., Madsen, B., Miller, S., and Sheikh, S. The Bank of Canada COVID-19 stringency index: measuring policy response across provinces.

[16] Cojocaru, M.-G., Bauch, C. T., and Johnston, M. D. Dynamics of vaccination strategies via projected dynamical systems. *Bulletin of mathematical biology 69*, 5 (2007), 1453.

[17] Daoust, J.-F., Bélanger, É., Dassonneville, R., Lachapelle, E., and Nadeau, R. Is the unequal covid–19 burden in canada due to unequal levels of citizen discipline across provinces? *Canadian Public Policy 48*, 1 (2022), 124–143.

[18] d'Onofrio, A., Manfredi, P., and Poletti, P. The impact of vaccine side effects on the natural history of immunization programmes: an imitation-game approach. *Journal of theoretical biology 273*, 1 (2011), 63–71.

[19] Ferguson, N. Capturing human behaviour. *Nature 446*, 7137 (2007), 733–733.

[20] Ferrante, G., Baldissera, S., Moghadam, P. F., Carrozzi, G., Trinito, M. O., and Salmaso, S. Surveillance of perceptions, knowledge, attitudes and behaviors of the italian adult population (18–69 years) during the 2009–2010 a/h1n1 influenza pandemic. *European journal of epidemiology 26*, 3 (2011), 211–219.

[21] Ferrante, L., Duczmal, L., Steinmetz, W., Almeida, A., Leão, J., Vassão, R., Tupinambás, U., and Fearnside, P. How brazil's president turned the country into a global epicenter of covid-19. *Journal of Public Health Policy 42* (2021), 439–451.

[22] Fields, R., Humphrey, L., Flynn-Primrose, D., Mohammadi, Z., Nahirniak, M., Thommes, E., and Cojocaru, M. Age-stratified transmission model of covid-19 in ontario with human mobility during pandemic's first wave. *Heliyon 7*, 9 (2021), e07905.

[23] Gauttam, P., Patel, N., Singh, B., Kaur, J., Chattu, V., and Jakovljevic, M. Public health policy of india and covid-19: diagnosis and prognosis of the combating response. *Sustainability 13*, 6 (2021), 3415.

[24] Hale, T., Anania, J., Angrist, N., Boby, T., Cameron-Blake, E., Di, M., Lucy, F., Goldszmidt, E. R., Hallas, L., Kira, B., Luciano, M., Majumdar, S., Nagesh, R., Petherick, A., Phillips, T., Tatlow, H., Webster, S., Wood, A., and Zhang, Y. Variation in government responses to COVID-19.

[25] He, W., Yi, G. Y., and Zhu, Y. Estimation of the basic reproduction number, average incubation time, asymptomatic infection rate, and case fatality rate for COVID-19: Meta-analysis and sensitivity analysis. *Journal of Medical Virology* (2020).

[26] Humphrey, L., Thommes, E. W., Fields, R., Hakim, N., Chit, A., and Cojocaru, M. G. A path out of COVID-19 quarantine: an analysis of policy scenarios. *medRxiv* (April 2020), 2020.04.23.20077503.

[27] Ibuka, Y., Li, M., Vietri, J., Chapman, G. B., and Galvani, A. P. Free-riding behavior in vaccination decisions: an experimental study. *PloS one 9*, 1 (2014), e87164.

[28] Lau, J., Yang, X., Tsui, H., and Kim, J. Monitoring community responses to the sars epidemic in hong kong: from day 10 to day 62. *Journal of Epidemiology & Community Health 57*, 11 (2003), 864–870.

[29] Li, J. Effects of behavior change on the spread of aids epidemic. *Mathematical and computer modelling 16*, 6-7 (1992), 103–111.

[30] Little, N., 2020.

[31] Lyons, J. The independence of ontario's public health units: does governing structure matter? *Healthcare Policy 12*, 1 (2016), 71.

[32] Mizumoto, K., Kagaya, K., Zarebski, A., and Chowell, G. Estimating the asymptomatic proportion of coronavirus disease 2019 (COVID-19) cases on board the diamond princess cruise ship, yokohama, japan, 2020. *Eurosurveillance 25*, 10 (Mar. 2020).

[33] Mohammadi, Z., Cojocaru, M. G., and Thommes, E. W. Human behaviour , NPI and mobility reduction effects on COVID-19 transmission in different countries of the world.

[34] Nash, J. F., et al. Equilibrium points in n-person games. *Proceedings of the national academy of sciences 36*, 1 (1950), 48–49.

[35] Nyabadza, F., Mukandavire, Z., and Hove-Musekwa, S. Modelling the hiv/aids epidemic trends in south africa: Insights from a simple mathematical model. *Nonlinear Analysis: Real World Applications 12*, 4 (2011), 2091–2104.

[36] Ontario, P. H. Covid-19 – what we know so far about... asymptomatic infection and asymptomatic transmission, 2020.

[37] Ontario, P. H. Health services locator map, February 2021.

[38] Osborne, M. J., and Rubinstein, A. *A Course in Game Theory*. The MIT Press, Cambridge, Massachusetts, 1994.

[39] Pelley, L. Several southern ontario covid-19 patients airlifted to northern hospitals, 2021.

[40] Prem, K., Cook, A. R., and Jit, M. Projecting social contact matrices in 152 countries using contact surveys and demographic data. *PLoS computational biology 13*, 9 (2017), e1005697.

[41] Price, D., Shearer, F., Meehan, M., McBryde, E., Moss, R., Golding, N., Conway, E., Dawson, P., Cromer, D., Wood, J., Abbott, S., McVernon, J., and , J. Early analysis of the australian covid-19 epidemic. *eLife 9* (2020), e58785.

[42] Rubin, G. J., Amlôt, R., Page, L., and Wessely, S. Public perceptions, anxiety, and behaviour change in relation to the swine flu outbreak: cross sectional telephone survey. *Bmj 339* (2009).

[43] Stutt, R. O., Retkute, R., Bradley, M., Gilligan, C. A., and Colvin, J. A modelling framework to assess the likely effectiveness of facemasks in combination with lock-down in managing the COVID-19 pandemic. *Proceedings of the Royal Society A 476*, 2238 (2020).

[44] Suwanprasert, W. Covid-19 and endogenous public avoidance: insights from an economic model. *Available at SSRN 3565564* (2020).

[45] Tuite, A. R., Fisman, D. N., and Greer, A. L. Mathematical modelling of covid-19 transmission and mitigation strategies in the population of ontario, canada. *CMAJ 192*, 19 (2020), E497–E505.

[46] Tully, S., Cojocaru, M., and Bauch, C. T. Coevolution of risk perception, sexual behaviour, and hiv transmission in an agent-based model. *Journal of theoretical biology 337* (2013), 125–132.

[47] Verelst, F., Willem, L., and Beutels, P. Behavioural change models for infectious disease transmission: a systematic review (2010–2015). *Journal of The Royal Society Interface 13*, 125 (2016), 20160820.

[48] Von Neumann, J., and Morgenstern, O. Theory of games and economic behavior. In *Theory of games and economic behavior*. Princeton university press, 2007.

[49] Wu, J., Tang, B., Bragazzi, N. L., Nah, K., and McCarthy, Z. Quantifying the role of social distancing, personal protection and case detection in mitigating COVID-19 outbreak in ontario, canada. *Journal of Mathematics in Industry 10*, 1 (May 2020).

[50] Zhong, W., Kim, Y., and Jehn, M. Modeling dynamics of an influenza pandemic with heterogeneous coping behaviors: case study of a 2009 h1n1 outbreak in arizona. *Computational and Mathematical Organization Theory 19* (2013), 622–645.

8. Appendix

8.1. Google Mobility Data

Google creates these aggregated and anonymized data sets from users who have turned on and agreed to share the information from their location history setting of their Google accounts on their phones [3]. As such, these data sets may not be representative of the population, especially in more rural settings with bad data reception or regions where cellphone usage is lower. Additionally, Google has not publicly shared the precise methodologies for calculating these social mobility scores, thus there is a certain degree of ambiguity as to how representative this data is of true population trends. We discuss this limitation more extensively in Chapter **??**. However, through data provided by Statistics Canada, the number of individuals with personal cell phones in Canada as of 2020 was above 80% [6]. Additionally, through data provided by Statista, Google Maps is the most downloaded mapping app in the United States, hence it is the most indicative mobility application for Canadian usage [14].

Some manipulation of Google mobility data was required to reconcile differences in geography and data recording. Ontario has 49 census divisions and six health regions (North East, North West, East, Central, Toronto, and West) that are further refined into 34 public health units (PHUs). In general, PHUs correspond to census borders, with smaller and less densely populated regions combining to form singular PHUs. In these cases the social mobility indicators were averaged across the census divisions making up each PHU. Additionally, the large census division of Kenora spans the northern PHUs of Northwestern (NWR), Thunder Bay (THB) and Porcupine (PQP) near equally. Given that the largest proportion of Kenora's population falls within NWR, we assign the mobility data for Kenora to this region and combine it with Rainy River division. Table 3 outlines the 51 Google mobility data collection regions and to which of the 34 Ontario public health units they were assigned.

8.2. Stringency index

The Bank of Canada (BoC) adapted the OxCGRT stringency index to create a stringency index of their own which is a measure of containment policies and public information campaigns [15]. More specifically, this index focuses on the economic impact of COVID-19. Similar to the OxCGRT, the BoC's stringency index does not measure the efficacy of a province's response

to COVID-19 nor does it provide a direct measure of the impact of government policies on the economy [15]. As of the summer 2020, researchers have been collecting publicly available information on government policies, creating daily government response indexes for all 10 provinces. With this, the bank could systematically measure, track and compare government policy responses. The BoC's stringency index follows the methodology of the OxCGRT with a few adjustments to make it more appropriate for the Canadian context and to capture specific differences in policy responses. In the BoC's stringency index, they added 3 policy indicators to the OxCGRT stringency index which included the following

- $C9$ - Restrictions on inter-provincial travel which splits the original OxCGRTs "internal movement restrictions" ($C7$) to capture only intra-provincial travel. Therefore adding this new $C9$ term gives greater weight to travel restrictions in the stringency index
- $C10$ - Enforcement mechanisms for individuals: OxCGRT does not include a measure identifying differences in provinces that have similar containment policies but different punishments or enforcement of these policies. This C10 indicator captures penalties for individuals violating public health orders
- $C11$ - Enforcement mechanisms for businesses violating public health orders

By adding more targeted dimensions, they increase the level of detail in the variation across provinces as well as over time. Additional geographical dimensions were included in the BoC index including types of outdoor events, outdoor versus indoor events and exceptions for certain travellers. Additionally, they refined the categories of coding values for several policy indicators based on a more detailed examination of policies in Canada. While they added categories to their indicators, the sub-index calculation decreases as the denominator in this equation increases

$$Sub - Index_j = 100 \times \left(\frac{a_j - \sum_{i=1}^{n} (\frac{1-f_{ij}}{n+1})}{b_j} \right) \tag{9}$$

- a_j is the ordinal value for the most restrictive measures in place within the province

- b_j is the maximum coding value
- n_j is the total number of targeting dimensions (e.g., by geography)
- f_{ij} is the flag for targeting dimension, i, which is equal to 1 if the policy is general or 0 if targeted

As a result of this increasing b term, often the sub-index is lower when compared with OxCGRT. While the BoC stringency index is better tailored to the Canadian landscape and the resulting economic implications, it does not provide a more refined scale and thus we still only have provincial data. Additionally, these factors which cater to the economic side of the stringency measures do not help us better fit our model to describe the behaviour of individuals in a given PHU. Thus we use the broader scope of the OxCGRT Stringency Index in our determination of the risk parameters.

Public Health Region	**Code**	**Google Mobility Regions**
Algoma Public Health	ALG	Algoma District
Brant County Health Unit	BRN	Brant County Brantford
Chatham-Kent Health Unit	CHK	Chatham-Kent
Durham Region Health Department	DUR	Regional Municipality of Durham
Eastern Ontario Health Unit	EOH	Prescott and Russel Stormont, Dundas and Glengarry
Grey Bruce Health Unit	GBC	Grey County Bruce County
Halton Region Health Department	HAL	Regional Municipality of Halton
Hamilton Public Health Services	HAM	Hamilton
Haldimand- Norfolk Health Unit	HDN	Haldimand County Norfolk County
Haliburton, Kawartha, Pine Ridge District Health Unit	HKP	Haliburton County Kawartha Lakes Northumberland County
Hastings and Prince Edward Counties Health Unit	HPE	Hastings County Prince Edward County
Huron Perth District Health Unit	HPH	Huron County Perth County
Kingston, Frontenac and Lennox and Addington Public Health	KFL	Frontenac County Lennox and Addington County
Lambton Public Health	LAM	Lambton County
Leeds, Grenville and Lanark District Health Unit	LGL	Lanark County Leeds and Grenville United Counties
Middlesex-London Health Unit	MID	Middlesex County
Niagara Region Public Health Department	NIA	Regional Municipality of Niagara
North Bay Parry Sound District Health Unit	NPS	Nipissing District Parry Sound District
Northwestern Health Unit	NWR	Rainy River District Kenora District
Ottawa Public Health	OTT	Ottawa
Southwestern Public Health	OXF	Oxford County Elgin County
Peel Public Health	PEL	Regional Municipality of Peel
Porcupine Health Unit	PQP	Cochrane District
Peterborough Public Health	PTC	Peterborough County
Renfrew County and District Health Unit	REN	Renfrew County
Simcoe Muskoka District Health Unit	SMD	Simcoe County Muskoka District Municipality
Sudbury and District Health Unit	SUD	Sudbury District
Thunder Bay District Health Unit	THB	Thunder Bay District
Toronto Public Health	TOR	Toronto
Timiskaming Health Unit	TSK	Timiskaming District
Region of Waterloo Public Health	WAT	Waterloo Regional Municipality
Wellington-Dufferin-Guelph Public Health	WDG	Wellington Dufferin
Windsor-Essex County Health Unit	WEC	Essex County
York Region Public Health Services	YRK	Regional Municipality of York

Table 3: PHU regions and their corresponding Google Mobility Regions